Computational Biology and Chemistry 74 (2018) 327–338

Contents lists available at ScienceDirect

Computational Biology and Chemistry

journal homepage: www.elsevier.com/locate/compbiolchem

Research Article

Targeting natural compounds against HER2 kinase domain as potential anticancer drugs applying pharmacophore based molecular modelling approaches

Shailima Rampogu, Minky Son, Ayoung Baek, Chanin Park, Rabia Mukthar Rana, Amir Zeb, Saravanan Parameswaran, Keun Woo Lee*

Division of Applied Life Science (BK21 Plus), Plant Molecular Biology and Biotechnology Research Center (PMBBRC), Systems and Synthetic Agrobiotech Center (SSAC), Research Institute of Natural Science (RINS), Gyeongsang National University (GNU), 501 Jinju-daero, Jinju 52828, Republic of Korea

ARTICLE INFO

Article history:
Received 19 February 2018
Received in revised form 2 April 2018
Accepted 4 April 2018
Available online 20 April 2018

Keywords:
HER2 inhibitors
Breast cancer
Natural compounds
Molecular dynamics

ABSTRACT

Human epidermal growth factor receptors are implicated in several types of cancers characterized by aberrant signal transduction. This family comprises of EGFR (ErbB1), HER2 (ErbB2, HER2/neu), HER3 (ErbB3), and HER4 (ErbB4). Amongst them, HER2 is associated with breast cancer and is one of the most valuable targets in addressing the breast cancer incidences. For the current investigation, we have performed 3D-QSAR based pharmacophore search for the identification of potential inhibitors against the kinase domain of HER2 protein. Correspondingly, a pharmacophore model, Hypo1, with four features was generated and was validated employing Fischer's randomization, test set method and the decoy test method. The validated pharmacophore was allowed to screen the colossal natural compounds database (UNPD). Subsequently, the identified 33 compounds were docked into the proteins active site along with the reference after subjecting them to ADMET and Lipinski's Rule of Five (RoF) employing the CDOCKER implemented on the Discovery Studio. The compounds that have displayed higher dock scores than the reference compound were scrutinized for interactions with the key residues and were escalated to MD simulations. Additionally, molecular dynamics simulations performed by GROMACS have rendered stable root mean square deviation values, radius of gyration and potential energy values. Eventually, based upon the molecular dock score, interactions between the ligands and the active site residues and the stable MD results, the number of Hits was culled to two identifying Hit1 and Hit2 has potential leads against HER2 breast cancers.

1. Introduction

Breast cancer (BC) is one of the common causes of death manifested in women worldwide (Shah and Rosso, 2014) accounting to 40,000 deaths annually in USA (Gajria and Chandarlapaty, 2011). Breast cancer incidences are relatively higher in the developed countries as compared to the under developed countries (Cleveland et al., 2012). This reflects the intrusion of the life style (Cauchi et al., 2016) in triggering the tumour development which includes physical activity (Wu et al., 2013) and obesity (Chan and Norat, 2015). Besides, exposure to radiations (Henderson et al., 2010; Ronckers et al., 2005) and family history (Tazzite et al., 2013; Melvin et al., 2016) may predominantly lead to cancer formation. Broadly cancer cells are represented by their receptors such as estrogen positive (ER+) and progesterone positive (PR+). Additionally, some breast cancers are characterized by elevated levels of growth promoting protein and are defined as HER2/neu(+) cancers. Fundamentally, human epidermal growth factor (HER) regulates the normal cell growth and its development and are comprised (Baselga, 2010) of transmembrane tyrosine kinase (TK) receptors such as epidermal growth factor receptors EGFR/ErbB1, HER2/ErbB2, HER3/ErbB3 and HER4/ErbB4 correspondingly (Hynes and Lane, 2005; Baselga and Swain, 2009; Gutierrez and Schiff, 2011; Baselga, 2010). Each receptor is a single glycoprotein (Iqbal and Iqbal, 2014) subunit that bears an extra cellular ligand binding domain, a transmembrane α-helix segment and intracellular tyrosine kinase domain(Li and Hristova, 2006). For proper exertion of their biological activities, receptor dimerization plays a key role which can be homodimerization or heterodimerization resulting in the

* Corresponding author.
E-mail address: kwlee@gnu.ac.kr (K.W. Lee).

https://doi.org/10.1016/j.compbiolchem.2018.04.002

autophosphorylation of the tyrosine residue located at the cytoplasmic domain. This mechanism leads to the initiation of a host of signalling pathways (Iqbal and Iqbal, 2014) stimulating several biochemical activities such as angiogenesis, invasion, cell differentiation, proliferation and survival (Iqbal and Iqbal, 2014). However, HER receptors generally remain inactive by avoiding dimerization (Baselga, 2010) and only specific dimers are implicated with cancers. HER2:HER3 heterodimer is regarded as being highly effective oncogenic unit because of the ligand induced tyrosine phosphorylation, interaction strength and downstream signalling (Amin et al., 2010). Additionally, HER2 demonstrates high catalytic activity and can undergo dimerization even without a ligand. Besides, HER2 confers an exposed open conformation of its dimerization domain and thus makes it an ideal partner (Gutierrez and Schiff, 2011). On the contrary, even though HER3 can bind to a ligand, its kinase domain is devoid of catalytic activity and hence relies on its partner for initiation of the signals (Garrett et al., 2003; Sierke et al., 1997; Guy et al., 1994; Dey et al., 2015). This makes the HER2:HER3 a pre-eminent dimer combination. HER2 dimerization additionally contributes to cell delocalization and the degradation of cell-cycle inhibitor $p27^{Kip1}$ resulting in cell-cycle progression (Citri and Yarden, 2006; Olayioye, 2001; Iqbal and Iqbal, 2014).

Nevertheless, HER2 displays a major role as a prime contributor to BC and its overexpression is demonstrated in 30% of early breast cancer cases (Lee-Hoeflich et al., 2008; Li et al., 2016). More specifically, the aberrant raise in the protein levels or its expression is associated with lymph node (+) and lymph node(−) breast cancers (Ross et al., 2009). Statistically, HER2 genes are elevated upto 25 ~50% and the amplified expression of HER2 is noticed in BC. Sequentially, nearly of about 2 million receptors are demonstrated at the surface of the tumour cells (Kallioniemi et al., 1992; Gutierrez and Schiff, 2011). Consequently, HER2 has been deemed trustworthy drug target in addressing HER2 (+) BCs. Besides BC, HER2 is also seen associated with ovarian (Menderes et al., 2017; Zanini et al., 2017) and gastric cancers (Rüschoff et al., 2012; Lucas and Cristovam, 2016).

Targeting HER2 has been a promising avenue to counter HER2 amplified breast cancer such as monoclonal antibodies and small molecules (Maximiano et al., 2016; Hynes and Lane, 2005; Schroeder et al., 2014). Trastuzumab, a monoclonal antibody (MB) that mechanistically acts by five different ways as reported earlier (Kute et al., 2004; Iqbal and Iqbal, 2014). Pertuzumab a humanized MB inhibits the activation of HER2 receptor duly impedes the dimerization of the receptor (Swain et al., 2015). This drug was also used in combination with trastuzumab (von Minckwitz et al., 2017) and docetaxel (Swain et al., 2015) in HER2-positive metastatic breast cancer. However, these treatments have manifested adverse effects such as infusion reactions, febrile neutropenia alopecia and diarrhea. Lapatinib a tyrosine kinase small molecule inhibitor operates by intervening with HER2 and EGFR pathways. However, it is effective when administered in combination with letrozole (Schwartzberg et al., 2010; Johnston et al., 2009). Lapatinib is credited with being the only approved orally active drug for patients with HER2-positive advanced breast cancers (Konecny et al., 2006; Li et al., 2016), while two synthetic chemical drugs namely dacomitinib and neratinib have made it to the Phase III trials (Gonzales et al., 2008; Kalous et al., 2012; López-Tarruella et al., 2012; Chan et al., 2016). However, prolonged administration of Lapatinib may induce drug resistance. This condition warrants a dire necessity for discovering new drug candidates as a majority of the incidences relapse (Li et al., 2016). Therapeutically, a small molecule hinders the process of tyrosine phosphorylation and thereby subsequent signalling events by challenging the ATP at the catalytic kinase domain and hence prevents aberrant amplification. Therefore, the objective of the current study is to identify novel potential natural compounds that can inhibit the undesirable amplification of HER2 signalling employing the 3D-QSAR based pharmacophore approach.

2. Materials and methods

2.1. Selection of the compounds

In order to generate the most reliable pharmacophore, the compounds that are involved in it play a very important role. For the current study, a total of 82 compounds have been chosen from different literatures (Hanan et al., 2016; Bryan et al., 2016; Cheng et al., 2016; Pannala et al., 2007; Liu et al., 2007; Gilson et al., 2016) that have demonstrated varied inhibitory activity values (IC_{50}) and were compiled into dataset. Prior to the commencement of the investigation the duplicates were removed for the explicit generation of the pharmacophore. Furthermore, the dataset was divided into the training set and the test set, correspondingly. Typically, a training set should consist of more than 16 compounds, wisely including the most active compound, should exhibit 4 order magnitudes and should be structurally distinct. Accordingly, 32 compounds were chosen as training set that demonstrated a wide range of IC_{50} values spanning between 0.003 nmol/L–25,000,000 nmol/L, Fig. 1. Additionally, the training set was divided into most active compounds displaying an inhibitory activity of less than or equal to 100 nmol/L, compounds demonstrating a range between 100 nmol//L and 10,000 nmol//L were labeled as moderately active and the compounds with IC_{50} above 10,000 were grouped into least active compounds. Subsequently, the 3D QSAR based pharmacophore was constructed using *HypoGen* algorithm implemented on the Discovery Studio (DS) v4.5, employing training set compounds. Likewise, the test set consists of 50 structurally diverse compounds were utilized to validate the generated pharmacophore model. The test set was further classified in the same order of magnitude as the training set compounds. Subsequently, their corresponding 2D structures were sketched using ChemSketch and were transferred to the Discovery Studio v4.5 (hereinafter DS) for processing the work further.

2.2. Ligand-based pharmacophore model generation

For the generation of the most potential pharmacophore models, the *Feature Mapping* protocol implemented on the DS was initiated to critically probe into the important chemical features imbibed within the training set compounds. The information rendered by the above was exploited in the generation of the pharmacophore. *3D QSAR Pharmacophore Generation* module available in the DS was employed to generate the pharmacophore using the Catalyst *HypoGen* algorithm. Additionally, the *best* algorithm was employed to generate the compounds with lower energy conformation at uncertainty value 3 having an interfeature distance of 2.97 at 95% confidence. For the generation of the pharmacophore the features such as Hydrogen Bond Acceptor (HBA), Hydrogen Bond Donor (HBD), Hydrophobic (HyP), Hydrophobic Aliphatic (HyA) and Ring Aromatic (RA) were chosen with a minimum of 0 and maximum of 5 features while retaining the remaining parameters as default. Correspondingly, the best pharmacophore from the generated was selected based upon the Debnath's analysis (Debnath, 2002; Debnath, 2003). According to Debnath's analysis, an ideal pharmacophore should essentially display a high correlation coefficient, least cost value and lowest RMSD.

2.3. Validation of the pharmacophore

The best pharmacophore model selected from the generated hypothesis was then subjected to validation performed by Fischer's

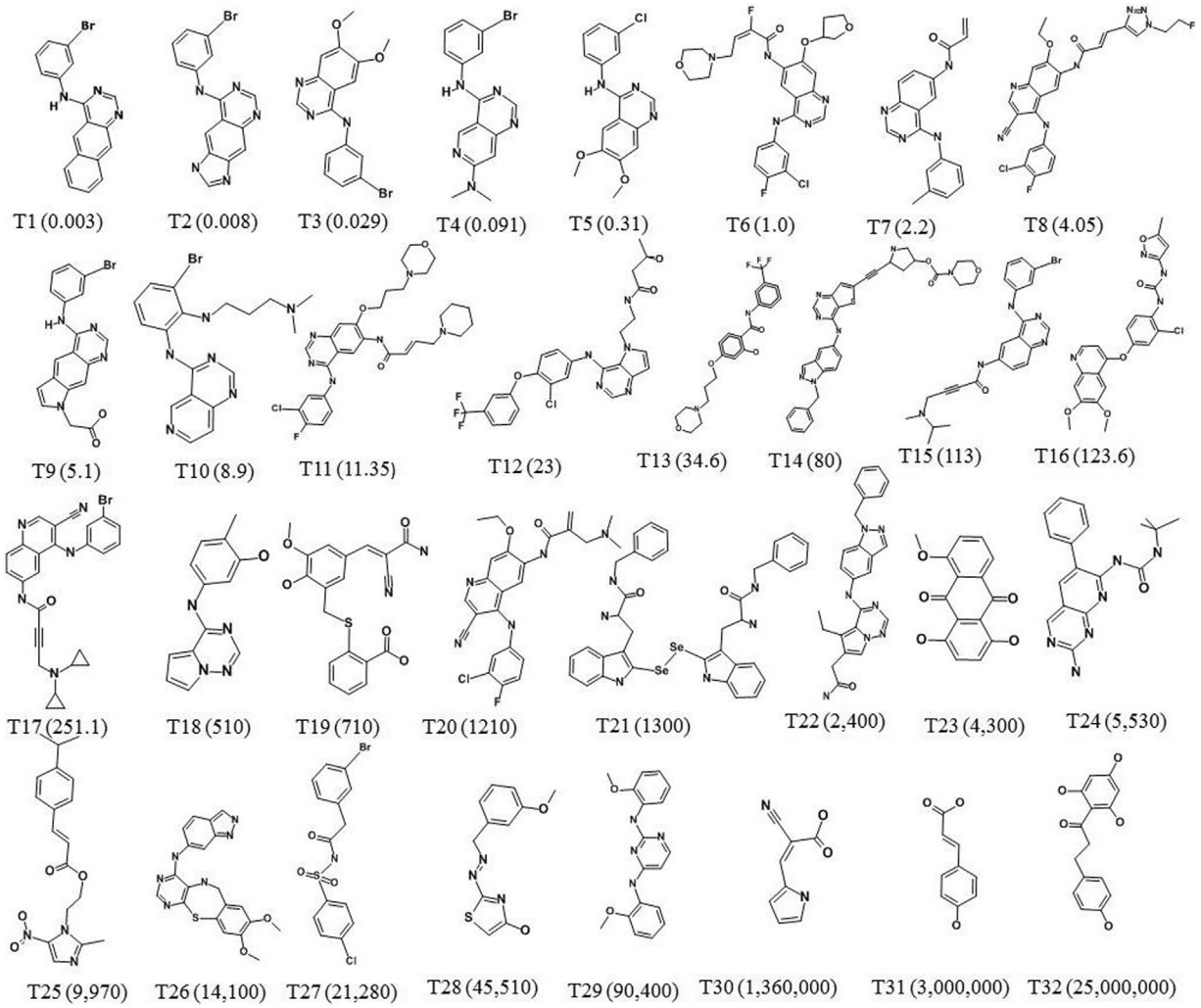

Fig. 1. 2D structures of 32 training set compounds utilized for the pharmacophore generation along with their IC_{50} values (nmol/L) indicated in parenthesis.

randomization method, test set method and decoy set method to assess its ability in differentiating the active compounds from the inactive compounds. Fischer's randomization approach was adapted to assess the statistical significance of the chosen hypothesis at 95% confidence level. This method additionally servers to affirm the selected pharmacophore was not generated by chance. The test set method of validation was employed to evaluate the capability of the pharmacophore model in identifying the compounds other than the training set with the same magnitude as the experimental activities. The test set validation was conducted utilizing the *Ligand Pharmacophore Mapping* protocol. Additionally, the decoy set method was recruited to further affirm the robustness of the model and was computed applying the formula (Rampogu et al., 2018)

$$EF = \left(\frac{Ha}{Ht}\right) \div \left(\frac{A}{D}\right)$$

$$GF = \left[\left(\frac{Ha}{4HtA}\right)\right](3A + Ht) \times [1 - (Ht - Ha) \div (D - A)]$$

Where D represents the total molecules in the data set, A indicates the total number of active molecules in the data set, Ht denotes the total number of Hits retrieved and Ha refers to the number of actives present in the retrieved Hits. Furthermore, the efficacy of the Hypo1 was determined by the goodness of fit score (GF) and the enrichment factor (EF), respectively. The GH score may range between 0 and 1, with 0 being null model while 1 representing a model to be exemplary (Fei et al., 2013; Hevener et al., 2009).

2.4. Database screening and drug-like assessment

Virtual small molecule database screening is one of the most elegant techniques adapted in the modern day drug discovery to obtain potential drug candidates for the corresponding diseases. For the current investigation, pharmacophore based virtual screening was performed considering the validated pharmacophore Hypo1 has the 3D query. The 3D query logically should possess all the bioactive functional features that are required by a potential drug candidate. Universal Natural Products Database (UNPD) (Gu et al., 2013) was employed for screening and subsequently to retrieve the candidate molecules. UNPD consists of 197,201 chemical compounds derived from animals, plants and microorganism. Nature has always been an attractive source of medicines from the ancient era and was foremost important in the folk medicine. *Ligand Pharmacophore Mapping* module implemented on the DS was employed opting the *fast rigid* options while retaining the other options as default. Correspondingly, all the compounds that have been successfully mapped with the features of the pharmacophore were regarded as potential candidates. The retrieved compounds were subjected to Lipinski's Rule of Five (RoF) (Lipinski, 2004) and ADMET properties

(Tareq Hassan Khan, 2010) to secure their drug-like criteria. For the current study an upper limit of 3, 3 and 0 was fixed for blood brain barrier (BBB), solubility and absorption respectively. RoF unequivocally acknowledges a compound to be well absorbed when it has less than 5 hydrogen bonds and log*P* values of less than 5. The molecular weight of the prospective drug candidate should be less than 500 Da, and further contains less than 10 hydrogen bond acceptors and rotatable bonds. Those compounds that have obeyed the criteria were forwarded to molecular docking calculations.

2.5. Molecular docking calculations

Virtual screening based molecular docking has been accredited with one of the highly reliable methods for the successful determination of the identified lead candidates as potential drugs. Furthermore, this approach offers an advantage of assessing the Hits and their interactions with the key residues located at the active site of the target molecule. The Cdocker protocol available on the DS was recruited for the current study that was executed simultaneously with CHARMm ff. Corresponding results were evaluated based upon the −Cdocker interaction energies, higher the –Cdocker energies greater is the favourable binding between the protein and the ligand (Rampogu, 2016).

The target for the current study is 3POZ which is in complex with the TAK-285 (inhibitor) and has a resolution of 1.5 Å (Aertgeerts et al., 2011). The active site was chosen for all the atoms that are located 15 Å around the inhibitor. The protein was prepared by employing the *clean protein* module available on the DS. All the hetero atoms including the water molecules were removed and the hydrogen bonds were added utilizing the CHARMm ff. The lead candidates along with the reference compound (hereinafter the most active compound from the training set) were subjected to molecular docking. The retrieved ligands from the above steps were allowed to generate 50 conformations and were further clustered to obtain the reliable binding mode. Furthermore, based upon the highest dock score and the interactions between the key residues and the ligand, the best docked pose was thus determined. In order to assess the reliability of the docking results and to understand their stability, the chosen poses form the dock results were escalated to molecular dynamics simulations performed by GROMACS v5.0.6 (Van Der Spoel et al., 2005).

2.6. Molecular dynamics simulation studies

To further understand the binding stability and the conformational changes within the active site of a protein and to affirm the docking results, the best docked poses were taken has initial structures for the MD analysis executed for 50 ns. GROMACS v5.0.6 (Van Der Spoel et al., 2005) was employed for its accomplishment adapting CHARMm ff (Van Der Spoel et al., 2005) and the ligand topologies were generated recruiting SwissParam (Zoete et al., 2011). The system was solvated with dodecahedron water box and the counter ions were subsequently added to neutralize the system. Steepest descent algorithm was employed to remove the bad contacts from the initial structures and were further subjected to equilibration by NVT and NPT, respectively. First equilibration was conducted at constant volume (NVT) for 1 ns at constant temperature of 300 K using Berendsen thermostat algorithm. Subsequently the second equilibration was executed for 1 ns at constant pressure (NPT) of 1 bar maintained by Parrinello-Rahman barostat (Parrinello, 1981). The molecular geometry of water and the hydrogen bonds involving atoms were constrain employing SETTLE (Miyamoto and Kollman, 1992) and LINCS (Hess et al., 1997). Particle Mesh Ewald (PME) (Darden et al., 1993) was employed to calculate long-range electrostatic interactions with a cut-off of 1.2 nm. The short-range non-bonded interactions were calculated within a cut-off of 1.2 nm. Additionally, a cut-off distance of 12 Å was attributed for Coulombic and van der Waals interactions. Each system was run for 50 ns saving the coordinates for every 2 fs. Correspondingly, the obtained results were evaluated using Visual Molecular Dynamics (VMD) (Humphrey et al., 1996) and DS.

3. Results

3.1. Generation of the pharmacophore model

The pharmacophore model was generated using the training set compounds employing *HypoGen* algorithm (Li et al., 2000), Fig. 1 selecting the feature driven by the *Feature Mapping Protocol* available on the DS. Accordingly, the Hydrogen Bond Acceptor (HBA), Hydrogen Bond Donor (HBD), Hydrophobic (HyP), Hydrophobic Aliphatic (HyA) and Ring Aromatic (RA) were chosen. Subsequently, 10 hypotheses were generated bestowed with five selected features. During the generation of the pharmacophore models, three different cost values were additionally generated. The fixed cost and the null cost were employed to judge the quality of the generated pharmacophore (John et al., 2010). The fixed cost refers to the cost of theoretical hypothesis that can predict the activity of the training set compounds with marginal deviation (John et al., 2010; Sakkiah et al., 2010). The null cost represents the cost of hypothesis devoid of features that approximates every activity to be an average activity. In order to generate the statistically reliable model above 90%, the difference between the two costs should lie $\geq$70 bits (Sakkiah et al., 2010). Besides configuration cost, correlation coefficient and the RMSD are the other parameters used to estimate the quality of the pharmacophore. Predominantly, the configuration cost of the most reliable pharmacophore should be less than 17 as it denotes the complexity of the hypothesis (John et al., 2010). The RMSD on the other hand delineates on the quality of the correlation that exists between the experimental and the estimated activity values (John et al., 2010; Sakkiah et al., 2010).

Among the generated 10 hypotheses, a four featured Hypo1 consisting of hydrogen bond acceptor (HBA), ring aromatic (RA) and two hydrophobic (HyP) features was determined as the best pharmacophore as it obeyed to Debnath's criteria. Accordingly, Hypo1 was conferred with highest cost difference (219.42), least root mean square deviation (RMSD) of 2.35, increased fit value (13.70) which were further complimented by the correlation coefficient of 0.88, Table 1 and Fig. 2. Moreover, two features namely HBA and RA have been retrieved from all the hypotheses notifying their key role in the inhibition of HER2. Additionally, the most active compound and the least active compound from the training set have been overlaid onto the Hypo1. It was noted that the most active compound has aligned with all the features of the pharmacophore, Fig. 2B while the least active compound has aligned with merely three features, Fig. 2C.

In order to further access the predictive ability of Hypo1, the regression analysis was performed over the training set compounds. The training set compounds were classified into most active, moderately active and least active compounds according to their IC_{50} values. The compounds with IC_{50} values less than 100 nmol/L were labeled as active, the compounds with IC_{50} values between 100 nmol/L–10,000 nmol/L were called as moderately active and the compounds with IC_{50} values >than 10,000 nmol/L were referred to as inactive compounds, respectively. It was noted that only two compounds were estimated inaccurately by the Hypo1. Two moderately active compounds were evaluated as active and least active compounds respectively, Table 2. This implies that Hypo1 was efficient in evaluating the activites of the

Table 1
Tabular column illustrating the details of the top ten hypotheses generated employing *HypoGen*.

Hypo no	Total cost	Cost difference	RMSD[a]	Correlation	Features[b]	Maximum fit
Hypo1	219.91	219.42	2.35	0.88	HBA, HyP, HyP, RA	13.70
Hypo2	225.15	286.19	2.45	0.87	HBA, HyP, HyA, RA	13.02
Hypo3	226.93	284.40	2.48	0.86	HBA, HyP, HyA, RA	12.71
Hypo4	229.23	282.10	2.50	0.86	HBA, HyP, HyP, RA	12.86
Hypo5	229.38	281.95	2.53	0.86	HBA, HyP, HyP, RA	12.21
Hypo6	229.47	281.86	2.54	0.86	HBA, HyP, HyA, RA	11.86
Hypo7	229.77	281.56	2.54	0.86	HBA, HyP, HyP, RA	12.21
Hypo8	230.63	280.70	2.56	0.86	HBA, HyP, HyA, RA	11.90
Hypo9	238.22	273.11	2.66	0.84	HBA, HyP, HyA, RA	11.55
Hypo10	240.60	270.74	2.69	0.84	HBA, HyP, HyA, RA	11.42

[a] Cost difference between the null and the total cost. The null cost, the fixed cost and the configuration cost are 511.33, 120.33 and 11.57 respectively.
[b] Abbreviation used for features: root mean square deviation (RMSD); hydrogen bond acceptor (HBA), Hydrophobic (HyP), Hydrophobic Aliphatic (HyA) and Ring Aromatic (RA), respectively.

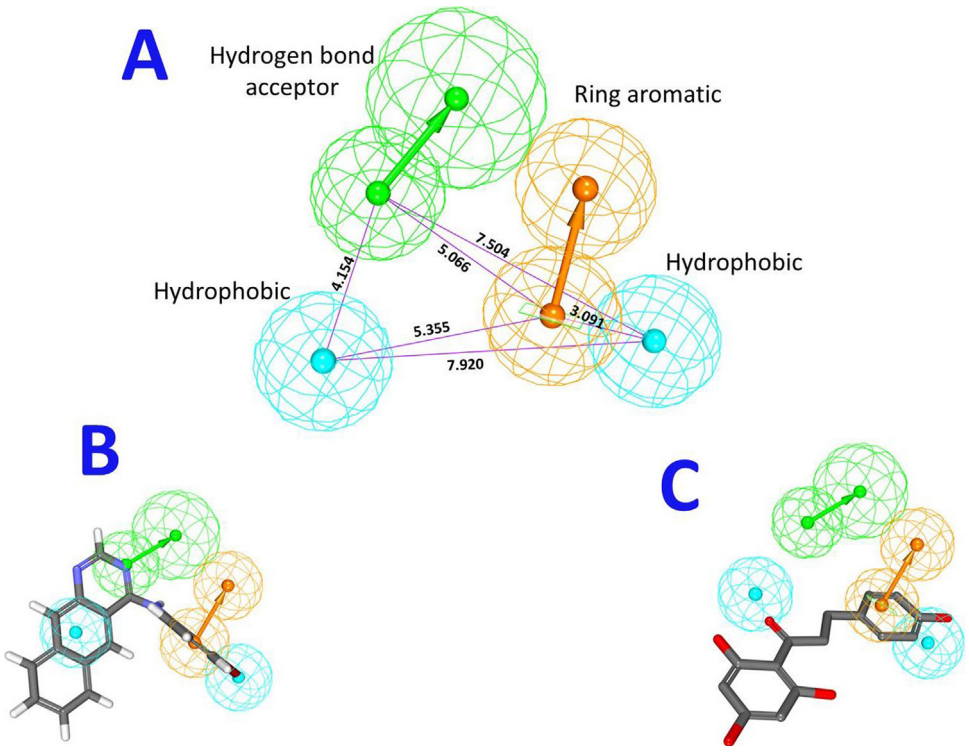

Fig. 2. *HypoGen* guided generated pharmacophore model with four features such as hydrogen bond acceptor (HBA), ring aromatic (RA), and two hydrophobic features (HyP). (A) The chosen four featured pharmacophore model Hypo1 with its geometry. (B) Most active compound from the training set is aligned to all the features of Hypo1. (C) Inactive compound from the training set is noticed to align with only three features.

compounds in their own activity ranges. Additionally, the reliability of the generated Hypo1 was assessed employing the Fischer's validation, test set method and the decoy set method.

3.2. Validation of the pharmacophore hypo1

Prior to the database screening for subsequent retrieval the chemical compounds with therapeutic ability, it is essential to understand the robustness of the pharmacophore model. Therefore, the validation of Hypo1 was performed by Fisher's randomization, test method and decoy set method.

3.2.1. Fischer's randomization method

Fischer's randomization was implemented to understand the significance of Hypo1 thereby assessing the correlation between the molecules and their corresponding activites. The statistical significance was calculated employing the formula (Sakkiah et al., 2010)

$$100\ [1 - (1 + X/Y)]$$

Here, X denotes the sum of all the hypothesis representing a total cost value lower than the Hypo, Y represents the sum of all the HypoGen runs (initial + random runs), Y = (19 + 1)

$$S = [1 - ((1 + 0)/19 + 1)]] \times 100\% = 95\%$$ (Sakkiah et al., 2010)

Correspondingly, 19 random spreadsheets were generated for ten pharmacophore models. Among them, Hypo1 represented the least cost value thereby illuminating its significance. Furthermore, it can be implied that the Hypo1 was far more superior and was not generated arbitrarily, Fig. 3A.

3.2.2. Test set method

Test set method imparts knowledge on the ability of the pharmacophore in determining the active compounds apart from the training set compounds (Sakkiah et al., 2010; Zhao et al., 2011). To achieve this, 50 known inhibitors other than the training set

Table 2
Estimated and the experimental activity values of the training set according to Hypo1.

Name	Fit	Estimate IC_{50} nmol/L	Activity IC_{50} nmol/L	Error[a]	Experimental scale[b]	Predictive scale[b]
1	13.47	0.77	0.003	280	+++	+++
2	13.37	0.82	0.008	130	+++	+++
3	13.43	0.85	0.029	32	+++	+++
4	12.98	0.85	0.091	29	+++	+++
5	13.51	0.86	0.32	2.4	+++	+++
6	13.48	0.88	1	−1.2	+++	+++
7	13.17	0.92	2.2	−1.3	+++	+++
8	11.33	1.1	4	28	+++	+++
9	13.47	1.7	5.1	−6	+++	+++
10	12.92	1.8	8.9	−3	+++	+++
11	13.45	2.6	11	−13	+++	+++
12	13.46	3	23	−27	+++	+++
13	10.73	78	35	14	++	+++
14	10.16	120	80	21	++	+++
15	13.15	200	110	−64	++	++
16	11.09	240	120	1.6	++	++
17	11.51	470	250	−3.2	++	++
18	10.52	500	510	1.5	++	++
19	11.01	520	710	−2.9	++	++
20	10.7	740	1200	−2.4	++	++
21	10.68	810	1300	−2.5	++	++
22	9.84	1000	2400	1.5	++	++
23	8.98	1100	4300	6.1	++	++
24	9.36	1700	5500	1.9	++	++
25	10.38	3600	10000	−9.5	++	++
26	10.37	4600	14000	−13	++	+
27	10.49	11000	21000	−26	+	+
28	9.19	16000	46000	−2.8	+	+
29	9.73	26000	90000	−20	+	+
30	6.74	250000	1400000	3.3	+	+
31	6.09	4500000	3000000	6.7	+	+
32	7.99	20000000	25000000	−99	+	+

[a] Error, ratio of the predicted activity (Pred IC50) to the experimental activity (Exp IC50) or its negative inverse if the ratio is <1.
[b] IC_{50} values ≤100 nmol/L are most active (+++), IC_{50} values between 100 nmol/L–10,000 nmol/L are moderately active (++) and IC_{50} values >10,000 nmol/L are least active compounds (+).

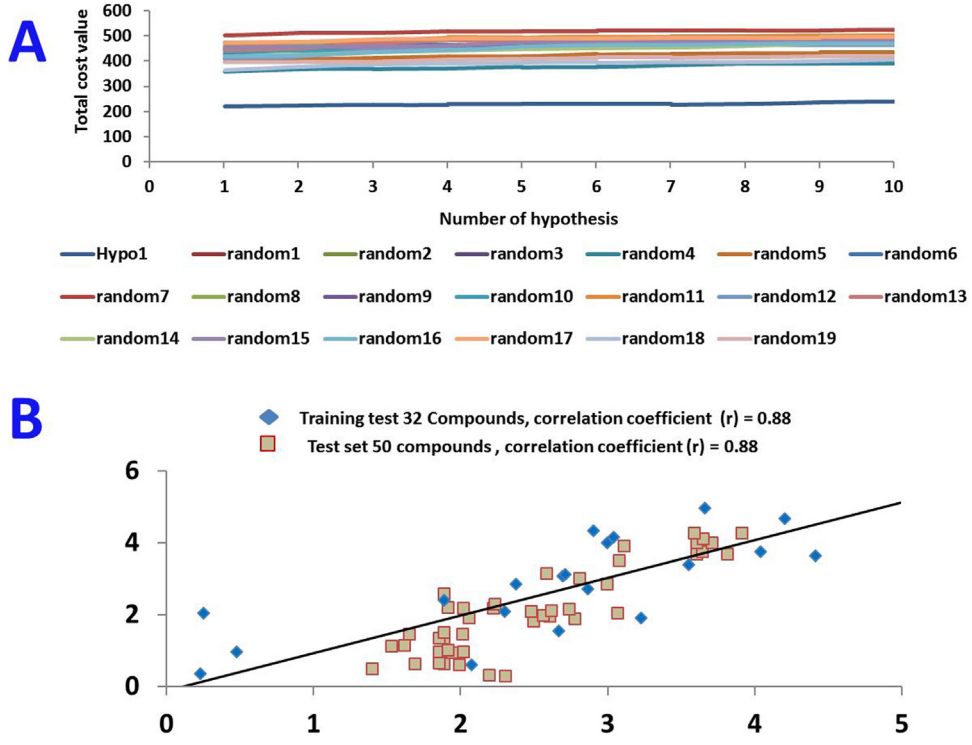

Fig. 3. Validation of Hypo1 employing Fischer's randomization and the test set method. (A) Difference in total cost between Hypo1 and 19 scrambles at confidence level 95%. (B) Correlation profiles determined by Hypo1 between the predicted and the experimental activities.

were chosen and the same protocol was employed as was with the training set compounds. The test set compounds were categorized in accordance with the training set compounds as most active, displaying an inhibitory activity of less than or equal to 100 nmol//L, compounds demonstrating a range between 100 nmol//L and 10,000 nmol//L as moderately active and the compounds with IC_{50} above 10,000 were labeled as least active. Subsequently, Hypo1 was efficient in categorizing the test compounds according to their activity ranges, Supplementary Table S1. However, one least active compound was over estimated as active compound. Additionally, it can be observed that the Hypo1 has demonstrated a high correlation (0.88) between the training set and the test set compounds as depicted in Fig. 3B.

3.2.3. Decoy set method of validation

The validation of the Hypo1 was further extended to investigate its potential in retrieving the inhibitors specific to the target molecule as performed in the decoy set method. Accordingly, an external database of 82 (D) compounds, Supplementary Table S2, was instituted consisting of 32 actives (A). The database screening was then initiated employing the *Ligand Pharmacophore Mapping* applying the *Best* algorithm module available in DS. This resulted in the procurement of 31 Hits (Ht) with 30 actives (Ha). The corresponding GH value was computed to be 0.87 illuminating the superior quality of the pharmacophore. The detailed calculations of the decoy set are tabulated in Table 3.

3.3. Database sieving for subsequent identification of lead compounds

The validated pharmacophore model, Hypo1 was then subjected to screen the databases to obtain the drug-like chemical compounds. Universal Natural Compound Database (UNPD) was employed for screening of the candidate compounds. By default nature is bestowed with large therapeutic value existing in animals, plants and even microorganisms. The current database UNPD comprises of 197,201 chemical compounds obtained from different natural sources which can be freely accessed.

The validated pharmacophore was allowed to redeem the compounds that have been complied with the pharmacophore features. Prior to the commencement of the screening process, a drug-like dataset was prepared considering the Lipinski's Rule of 5 (Ro5) and ADMET. Ro5 fundamentally defines the molecular properties of a given compound that are decisive in determining the pharmacokinetics of a drug. The obtained 86,001 compounds were further filtered considering a fit value above 10. The resultant molecules were subjected to *Ligand Pharmacophore Mapping* which mapped to 5030 compounds. The retrieved drugs were further forwarded to docking mechanism along with the training set compounds to ascertain the prospective drug candidates and additionally to evaluate the quintessential binding mode. The detailed screening mechanism has been presented in pictorial depiction, Fig. 4.

Table 3
Different factors computed by Hypo1 in the decoy set validation method. The obtained GF score ensures the predictive ability of Hypo1.

Parameters	Values
Total number of molecules in database (D)	83
Total number of actives in database (A)	32
Total number of Hit molecules from the database (Ht)	31
Total number of active molecules in Hit list (Ha)	30
% Yield of active [(Ha/Ht) × 100]	96.77
% Ratio of actives [(Ha/A) × 100]	93.75
Enrichment Factor (EF)	2.67
False negatives (A-Ha)	2
False Positives (Ht–Ha)	1
Goodness of fit score (GF)	0.87

3.4. Molecular docking studies

Docking studies were performed to sample the small molecules at proteins binding pocket. The retrieved compounds along with the reference compound was subjected to molecular docking employing the Cdocker module accessible on the DS. To ensure the docking accuracy, the innate co-crystal was docked into the active site of the protein to generate an appropriate binding orientation. Accordingly, the pose cluster radius was defined as 0.1 Å. The random conformation steps were elected as 50 with 50 orientations to refine. Correspondingly, the simulated annealing and the include electrostatic interactions were determined as *true*. The docked pose has rendered and reasonable RMSD of 0.81 Å upon comparison with the cocrystal, Supplementary Fig. S1. Therefore, these parameters were further considered to evaluate the affinity of the screened compounds.

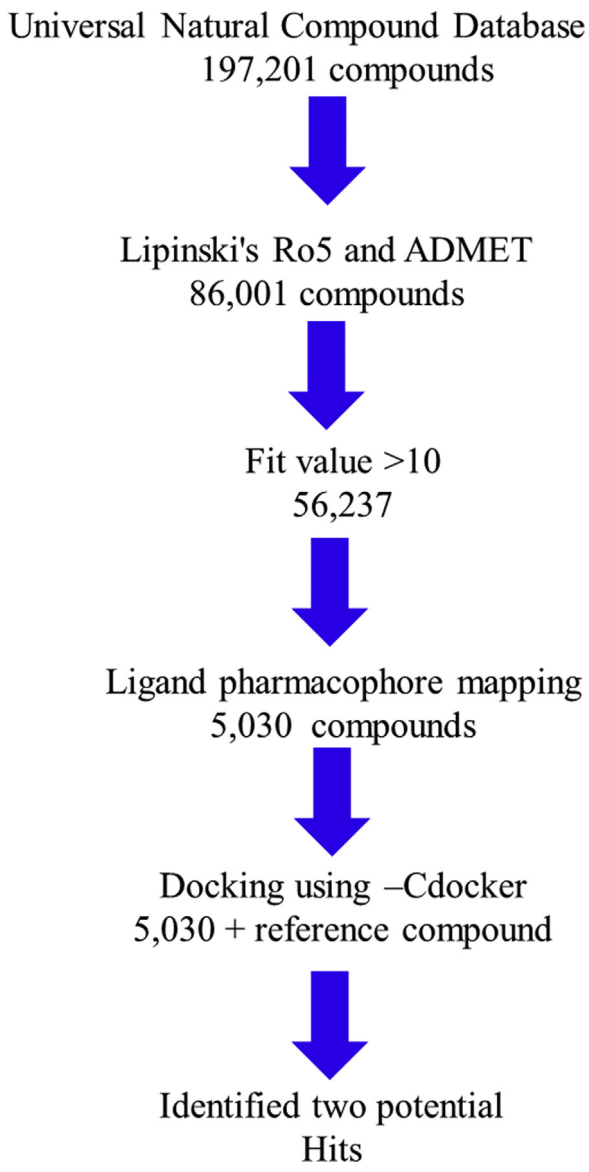

Fig. 4. Pictorial depiction of the steps involved in screening the UNP database to identify the most potential lead candidates.

Table 4
Corresponding dock results of the reference and the lead candidates calculated by the Cdocker protocol.

Compound name	–Cdocker energy	–Cdocker interaction energy
Reference	19.16	46.08
Hit1	20.45	65.41
Hit2	34.81	62.04

The docking results revealed that the reference compound has generated –Cdocker interaction energy of 46.08 and –Cdocker energy of 19.16 respectively. Therefore, this score is determined as the cut-off in choosing the lead candidates. Subsequently, 33 compounds have rendered higher dock score than the reference compound. These were further assessed manually for the hydrogen bond interactions and their binding mode analysis. Consequently, two compounds that have displayed the higher dock score than the reference were noticed to interact with the key residues located at the protein's binding pocket upon manual inspection, Table 4.The identified Hits have also found to map with all the pharmacophore features, Fig. 5. To further authenticate the reliability of the binding modes and to assess their binding stability, the compounds along with the reference were escalated to molecular dynamics (MD) simulations employing GROMACS v5.0.6.

3.5. Molecular dynamics simulations

To establish the results generated by docking and to understand the dynamic behaviour of the protein and ligand with each other, the MD simulation was executed across three systems. During the process of simulation, the protein-ligand complexes were assessed for the root mean square deviation (RMSD), radius of gyration (Rg) and the potential energy performed for 50 ns (Rampogu et al., 2017a; Rampogu et al., 2017b). The RMSD values computed for the protein backbone atoms ranged between 0.1 nm ~ 0.25 nm implying the systems were optimally converged, Fig. 6A. Marginal variations in RMSD during the initial runs were noticed due to the accommodation of the ligand in the proteins active site. However, after 15 ns no major variations were noticed. Furthermore, the average RMSD of the reference was observed to be 0.23 nm, while that observed for Hit1 and Hit2 was 0.20 nm and 0.22 nm, respectively, Fig. 6A. Additionally, the potential energy has reiterated the same demonstrating the systems were in harmony with no variations. The potential energy of the Hits was found to be between −559000 kJ/mol to 569000 kJ/mol as was observed with the reference compound, data not shown. The radius of gyration confers compactness of the systems and was noted that the three systems were compact and well folded without any aberrant behaviour, data not shown. Correspondingly, the representative structures from the last 10 ns trajectories were extracted to evaluate their binding modes. Upon subsequent superimposition of the representative structures, it was elucidated that the binding pattern of Hits were in agreement with the reference compound, Fig. 6B. It can further be understood that the Hits have lodged themselves in the active site of the protein, Fig. 6B, and are in agreement with the co-crystal, Supplementary Fig. S2. This finding additionally ensures the reliability of the docking protocol employed. Furthermore, it was disclosed that the ligands have been seated in the binding pocket showing interactions the key residues. From the knowledge gained by the crystal structure (3POZ), the key residues that contribute towards the inhibition were identified as Leu777, Thr790, Met793, Arg841, Thr854, Asp855 and Phe856 respectively. Delineating on the interactions exhibited by the compounds it can be understood that the reference has formed one hydrogen bond with Asp855 residue, Fig. 7. The other key residues such as Leu777, Arg841 and Thr854 have involved in the interaction by the van der Waals interactions, while Thr790 and Phe856 have formed the π-sigma and π-π T-shaped interactions, respectively, Supplementary Fig. S3. The Hits also have formed the essential interactions with the pivotal residues located at the binding pocket. Hit1 has formed two hydrogen bonds, one with Lys745 and the other with Phe856, Fig. 7. Besides, Leu777, Thr790, Met793, Thr854 and Asp855 have formed the van der Waals interactions firmly accommodating the

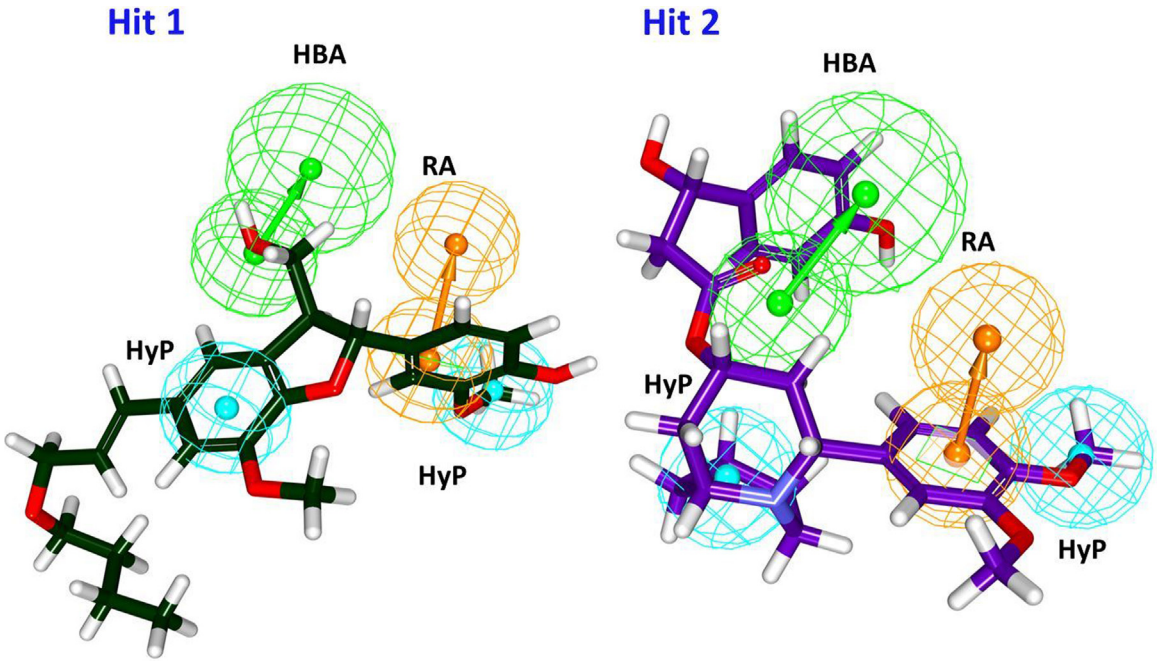

Fig. 5. Overlay of the Hits onto the pharmacophore model. The Hits were observed to map with all the pharmacophore features such as one hydrogen bond acceptor, one ring aromatic and two hydrophobic features.

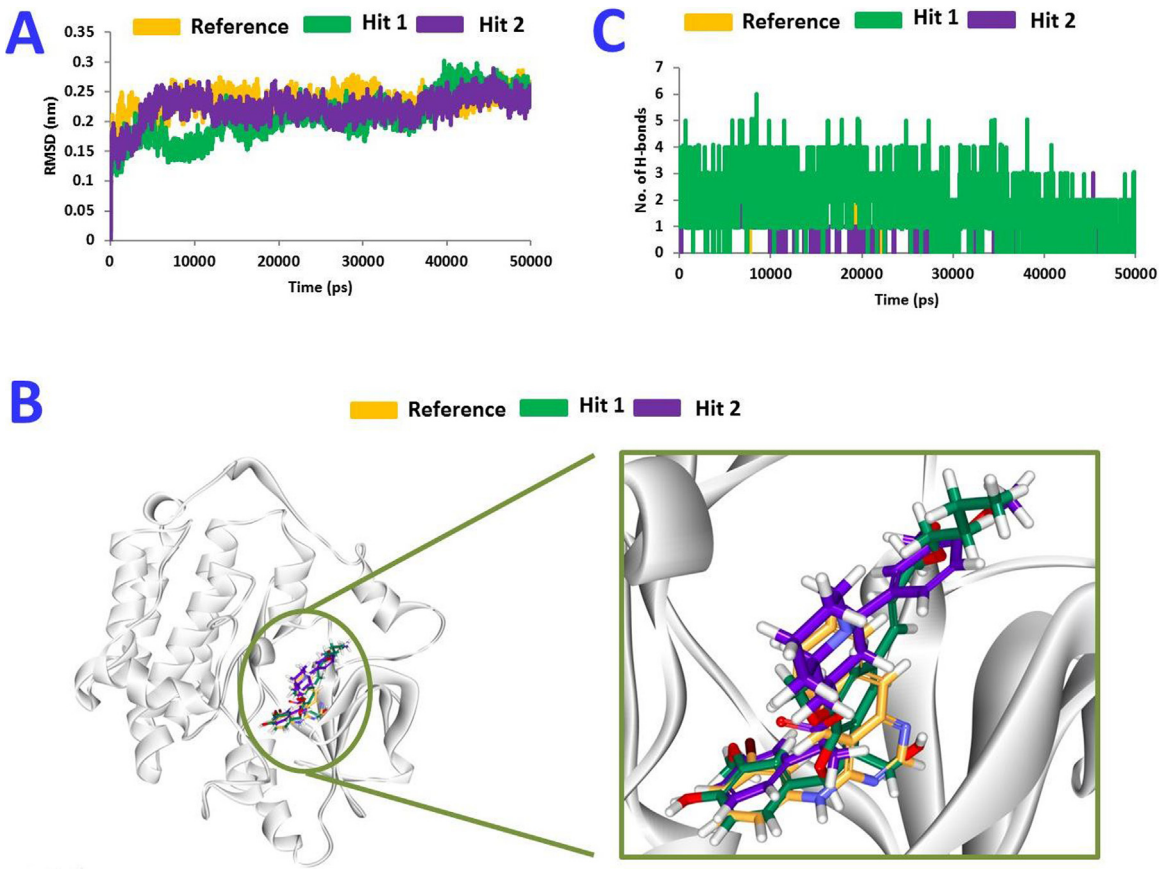

Fig. 6. Molecular dynamics simulation results obtained during 50 ns. (A) The root mean square deviation (RMSD) of the protein backbone. (B) Binding mode analysis of the reference and the Hits in the proteins active site. The Hits are found to obey the similar binding pattern as the reference. Picture of the left is the superimposed form and the picture on the right is its magnified form. (C) Monitoring the number of hydrogen bonds between the protein-Hits. The Hits have displayed consistency in rendering the hydrogen bonds throughout the simulations. Comparatively, the reference compound marginally shows the hydrogen bonds.

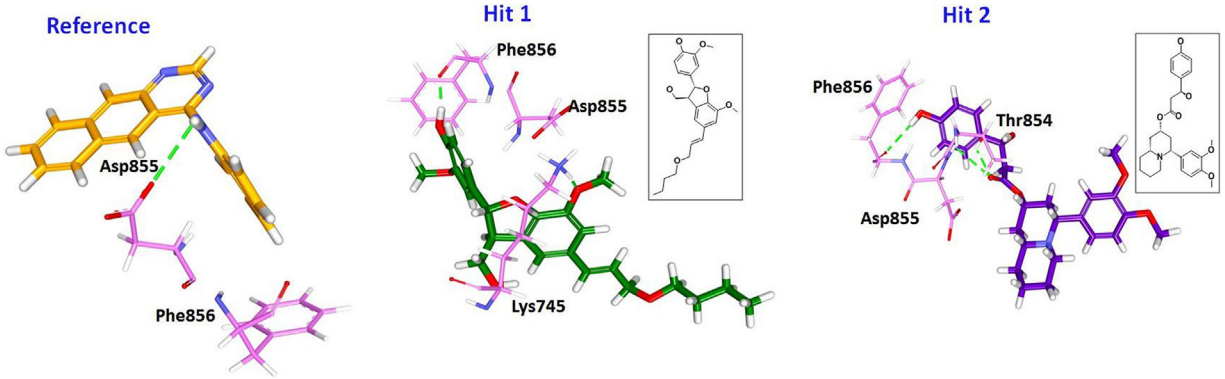

Fig. 7. The binding conformations and the hydrogen bond interaction of the reference and the Hits with the key residues of the protein. The hydrogen bonds are represented in green dotted lines and the protein residues are represented in pink stick model. The 2D structures of Hit1(A) and Hit2 (B) are represented in black box. (For interpretation of the references to colour in this figure legend, the reader is referred to the web version of this article.)

compound within the active site. Additionally, the residues Lys745 and Phe856 were observed to be involved in the interaction through the π bonds, Supplementary Fig. S3. The Hit2 has rendered three hydrogen bonds one each with Thr854, Asp855 and Phe856 respectively, Fig. 7. The key residue, Thr790 has anchored with the ligand by van der Waals interactions, Supplementary Fig. S3. The details of the residues and atoms that have participated in the inhibitory effect have been tabulated, Table 5 and Supplementary Fig. S3.

4. Discussion

The study was initiated to discover the potential lead candidate molecules that can effectively render their inhibitory activity on HER2 breast cancers. Breast cancer incidences have been increasing recently due to various reasons. Human epidermal growth factor receptor 2 (HER2) is one of causes of cancer predominantly seen associated with HER2 (+) breast cancers wherein the HER2 protein is overexpressed. One of the ideal ways to combat this

Table 5
Detailed molecular interactions between the protein-Hit complexes. The hydrogen bond interactions are demonstrated at the atom level.

Name	Hydrogen bond Interactions <3 Å	π-bonds	Alkyl/π- alkyl	van der Waals interactions
Ref	Asp855:OD1-H9 (2.9)	Thr90, Met766, Phe856	Val726, Ala743, Lys745, Cys775, Leu844, Leu858,	Ile744, Arg776, Leu777, Ile789, Cys797, Arg841, Asn842, Thr854
Hit1	Lys745: HZ3-O9 (1.8) Phe856:O-H48 (1.8)	Phe856,	Lys745	Leu718, Gly719, Ile744, Val769, Arg776, Leu777, Ile789, Thr790, Leu792, Met793, Gly796, Asp800, Leu844, Thr854, Leu858, Phe997
Hit2	Thr854: HG1-O23 (2.1) Asp855: HN-O23 (2.9) Phe856:O-H66 (2.4)	Phe856	Phe856	Gly719, Ala743, Lys745, Cys775, Arg776, Leu788, Thr790, Leu792, Pro794, Cys797, Leu844, Phe997, Leu1001

In parenthesis, the hydrogen bond length.

condition is to discover new drug candidates that can control its amplification.

For the current investigation, we hypothesized that targeting the HER2 protein with small molecules could correspondingly pave way for the inhibition of HER2 positive breast cancers. 3D-QSAR pharmacophore based drug discovery has gained popularity in identifying novel lead candidates as the discovery is based on the pharmacophore features furnished by the known inhibitors. This approach was presumed to retrieve molecules from the colossal databases imbibing the inhibitory traits conferred by the known inhibitors. Accordingly, a pharmacophore consisting of four features has been generated that was subsequently validated employing three different approaches. The validated pharmacophore, upon UNPD screening has retrieved two Hits that abide to all the features displayed by the Hypo1. This indicated that the retrieved Hits might possess the same or enhanced therapeutic ability corresponding to the known inhibitors.

Accordingly, the Hits were scrupulously assessed for their binding modes and their behaviour in the protein's active site to again further insight. The best poses from the docking results were escalated to the MD simulations. Resultant RMSD plots have indicated that the Hits have acted in accordance with the reference compound and have manifested no anomalous behaviour throughout the simulations. Precisely, the average RMSD profiles of the Hits and the reference conducted for the protein backbone atoms were detected to be below 0.25 nm implying that the systems were stable as was seen with the reference. Additionally contemplating on the Rg and potential energies reflect that the protein-Hit complexes were well compact and consistent throughout the simulations. The MD results principally infer the systems have shown no aberrant behaviour and were seated in the proteins binding pocket as was seen in the crystal structure, Supplementary Fig. S1. Therefore, the representative structures were further examined for their interactions with the key residues. Focusing on the hydrogen bond interactions, it can be deduced that the Hits have rendered greater number of hydrogen bonds as compared to the reference compounds, Fig. 6C complemented by uninterrupted bonds during 50 ns simulation run, Fig. 6C. The average hydrogen bond represented by the reference was noticed to be 0.99 while Hit1 has demonstrated 2.02 and Hit2 has represented 1.19, respectively. This finding supports our reasoning that the Hits might be potential inhibitors against HER2. We further speculated that the additional bonds such as electrostatic interactions and hydrophobic interactions might assist in firm positioning of the Hits within the active site of the protein besides inducing inhibitory effect. The residue Phe856 has constantly demonstrated the π-π T stacked interaction in the reference and the Hits respectively as was noticed in the crystal structure. The benzene ring of the Phe856 residue was shown to bind with the benzene ring of the inhibitor (TAK-85). Hit1 formed the π-π T stacked interaction with a distance of 5.5 Å while Hit2 displayed the interaction with a distance of 5.30 Å. This distance was in agreement with that of the reference and the co-crystal both of which have represented a distance of 5.5 Å. This leads us to hypothesize that the presence of benzene ring in the inhibitors and its positioning towards the inner groove of the active site (towards the Phe856) offers an enhanced inhibitory effect as was seen in the crystal structure and the reference. Similar types of interactions were observed with Val726 residue. The second benzene ring of the co-crystal has demonstrated a π- alkyl bond with CB atom Val726 rendered by 5.0 Å. Similarly, the CB atom Val726 has interacted with three benzene rings of the reference demonstrated by a bond distance of 5.2 Å, 4.5 Å and 4.9 Å, respectively. Delineating on the Hits, it can be noticed that the CB atom of Val726 participated in the π- alkyl with the Hit1 rendered by a distance of 4.5 Å and Hit2 with 5.0 Å, correspondingly. From the current findings, it can be established that the Val726 is located at the mouth of the active site and Phe856 is towards the inner groove of the active site, Supplementary Fig. S4. The interactions with these residues contribute to the accurate positioning of the ligand within the active site holding the ligands at both the ends. We further speculate that one or both of these residue interactions are imperative in proper accommodation of the ligands in the active site and subsequently contributing to effective therapeutics. Additionally, an analogy of the active site residue interaction between the reference and the Hits was conducted. It was vivid that the Hits have interacted with more number of active site residues than the reference, Supplementary Fig. S3 and Table 5. Additionally, Arg776 was critically involved with the reference and Hits and thus may play an important role in the therapeutic activity. These Hit compounds have additionally displayed acceptable pharmacokinetic properties and obeyed Ro5.

The cocrystal inhibitor TAK-285 has been credited with HER2/EGFR dual inhibitor. We further conjectured that the identified Hits might offer a similar inhibitory mechanism. However, the Hits were retrieved and assessed against a reference inhibitor having an IC_{50} value of 0.003 nmol//L. Corresponding results have demonstrated that the Hits could be promising than the reference compound in terms of dock scores, stable interactions with active residues and further augmented by the MD results. This IC_{50} value is far lower than the inhibitors that are current drugs in the clinical trials such as Lapatinib and cocrystal TAK-285. Accordingly, we speculate that the identified Hits might presumably be imbibed with greater efficacy. Taken together, we therefore suggest that the Hits could act has potential inhibitors against HER2 breast cancers.

5. Conclusion

Targeted therapy is one of the most effective therapeutic applications in treating cancers. Amongst which the small

molecule therapy has gained a wider recognition. In the current study a 3D-QSAR based database search was conducted to secure the potential small compounds. Subsequently, the validated four featured pharmacophore has retrieved two candidate molecules upon performing the pharmacophore search against UNP database. These chemical compounds were then assessed for their prospective effectiveness against HER2 using known inhibitor as a reference. Based upon the dock score, MD simulation studies, binding mode analysis and the interaction with the active site residues, we propose two candidates Hit1 (UNPD198940) and Hit2 (UNPD185256) from the UNP database as the candidate potential leads against HER2.

Conflict of interest

None.

Acknowledgements

This research was supported by the Pioneer Research Center Program (NRF-2015M3C1A3023028) through the National Research Foundation of Korea (NRF) funded by the Ministry of Science, ICT and Future Planning.

Appendix A. Supplementary data

Supplementary data associated with this article can be found, in the online version, at https://doi.org/10.1016/j.compbiolchem.2018.04.002.

References

Aertgeerts, K., Skene, R., Yano, J., Sang, B.-C., Zou, H., Snell, G., et al., 2011. Structural analysis of the mechanism of inhibition and allosteric activation of the kinase domain of HER2 protein. J. Biol. Chem. 286, 18756–18765.
Amin, D.N., Sergina, N., Ahuja, D., McMahon, M., Blair, J.A., Wang, D., et al., 2010. Resiliency and Vulnerability in the HER2-HER3 Tumorigenic Driver. Sci. Transl. Med. 2 16ra7–16ra7.
Baselga, J., Swain, S.M., 2009. Novel anticancer targets: revisiting ERBB2 and discovering ERBB3. Nat. Rev. Cancer 9, 463–475.
Baselga, J., 2010. Treatment of HER2-overexpressing breast cancer. Ann. Oncol..
Bryan, M.C., Burdick, D.J., Chan, B.K., Chen, Y., Clausen, S., Dotson, J., et al., 2016. Pyridones as highly selective, noncovalent inhibitors of T790M double mutants of EGFR. ACS Med. Chem. Lett. 7, 100–104.
Cauchi, J.P., Camilleri, L., Scerri, C., 2016. Environmental and lifestyle risk factors of breast cancer in Malta—a retrospective case-control study. EPMA J. 7, 20.
Chan, D.S.M., Norat, T., 2015. Obesity and breast cancer: not only a risk factor of the disease. Curr. Treat. Options Oncol..
Chan, A., Delaloge, S., Holmes, F.A., Moy, B., Iwata, H., Harvey, V.J., et al., 2016. Neratinib after trastuzumab-based adjuvant therapy in patients with HER2-positive breast cancer (ExteNET): A multicentre, randomised, double-blind, placebo-controlled, phase 3 trial. Lancet Oncol. 17, 367–377.
Cheng, H., Nair, S.K., Murray, B.W., Almaden, C., Bailey, S., Baxi, S., et al., 2016. Discovery of 1-{(3R,4R)-3-[({5-Chloro-2-[(1-methyl-1H-pyrazol-4-yl)amino]-7H-pyrrolo[2,3-d]pyrimidin-4-yl}oxy)methyl]-4-methoxypyrrolidin-1-yl} prop-2-en-1-one (PF-06459988), a potent, WT, sparing, irreversible inhibitor of T790M-containing EGFR mutants. J. Med. Chem. 59, 2005–2024.
Citri, A., Yarden, Y., 2006. EGF–ERBB signalling: towards the systems level. Nat. Rev. Mol. Cell Biol. 7, 505–516.
Cleveland, R.J., North, K.E., Stevens, J., Teitelbaum, S.L., Neugut, A.I., Gammon, M.D., 2012. The association of diabetes with breast cancer incidence and mortality in the Long Island Breast Cancer Study Project. Cancer Causes Control. 23, 1193–1203.
Darden, T., York, D., Pedersen, L., 1993. Particle mesh Ewald: an N·log(N) method for Ewald sums in large systems. J. Chem. Phys. 98, 10089.
Debnath, A.K., 2002. Pharmacophore mapping of a series of 2,4-diamino-5-deazapteridine inhibitors of mycobacterium avium complex dihydrofolate reductase. J. Med. Chem. Am. Chem. Soc. 45, 41–53.
Debnath, A.K., 2003. Generation of predictive pharmacophore models for CCR5 antagonists: study with piperidine- and piperazine-based compounds as a new class of HIV-1 entry inhibitors. J. Med. Chem. 46, 4501–4515.
Dey, N., Williams, C., Leyland-Jones, B., De, P., 2015. A critical role for HER3 in HER2-amplified and non-amplified breast cancers: function of a kinase-dead RTK. Am. J. Transl. Res. 7, 733–750.
Fei, J., Zhou, L., Liu, T., Tang, X.-Y., 2013. Pharmacophore modeling, virtual screening, and molecular docking studies for discovery of novel Akt2 inhibitors. Int. J. Med. Sci. 10, 265–275.
Gajria, D., Chandarlapaty, S., 2011. HER2-amplified breast cancer: mechanisms of trastuzumab resistance and novel targeted therapies. Expert Rev. Anticancer Ther. 11, 263–275.
Garrett, T.P.J., McKern, N.M., Lou, M., Elleman, T.C., Adams, T.E., Lovrecz, G.O., et al., 2003. The crystal structure of a truncated ErbB2 ectodomain reveals an active conformation, poised to interact with other ErbB receptors. Mol. Cell. 11, 495–505.
Gilson, M.K., Liu, T., Baitaluk, M., Nicola, G., Hwang, L., Chong, J., 2016. Binding DB in 2015: a public database for medicinal chemistry, computational chemistry and systems pharmacology. Nucleic Acids Res. 44, D1045–D1053.
Gonzales, A.J., Hook, K.E., Althaus, I.W., Ellis, P.A., Trachet, E., Delaney, A.M., et al., 2008. Antitumor activity and pharmacokinetic properties of PF-00299804, a second-generation irreversible pan-erbB receptor tyrosine kinase inhibitor. Mol. Cancer Ther. 7, 1880–1889.
Gu, J., Gui, Y., Chen, L., Yuan, G., Lu, H.Z., Xu, X., 2013. Use of natural products as chemical library for drug discovery and network pharmacology. PLoS One 8.
Gutierrez, C., Schiff, R., 2011. HER2: Biology, detection, and clinical implications. Arch. Pathol. Lab. Med. 135, 55–62.
Guy, P.M., Platko V, J.V., Cantley, L.C., Cerione, R.A., Carraway, K.L., 1994. Insect cell-expressed p180erbB3 possesses an impaired tyrosine kinase activity. Proc. Natl. Acad. Sci. U. S. A. 91, 8132–8136.
Hanan, E.J., Baumgardner, M., Bryan, M.C., Chen, Y., Eigenbrot, C., Fan, P., et al., 2016. 4-Aminoindazolyl-dihydrofuro[3,4-d]pyrimidines as non-covalent inhibitors of mutant epidermal growth factor receptor tyrosine kinase. Bioorg. Med. Chem. Lett. 26, 534–539.
Henderson, T.O., Amsterdam, A., Bhatia, S., Hudson, M.M., Meadows, A.T., Neglia, J.P., et al., 2010. Systematic review: surveillance for breast cancer in women treated with chest radiation for childhood, adolescent, or young adult cancer. Ann. Intern. Med. 444–455.
Hess, B., Bekker, H., Berendsen, H.J.C., Fraaije, J.G.E.M., 1997. LINCS: A linear constraint solver for molecular simulations. J. Comput. Chem. 18, 1463–1472.
Hevener, K.E., Zhao, W., Ball, D.M., Babaoglu, K., Qi, J., White, S.W., et al., 2009. Validation of molecular docking programs for virtual screening against dihydropteroate synthase. J. Chem. Inf. Model. 49, 444–460.
Humphrey, W., Dalke, A., Schulten, K.V.M.D., 1996. Visual molecular dynamics. J. Mol. Graph. 14, 33–38.
Hynes, N.E., Lane, H.A., 2005. ERBB receptors and cancer: the complexity of targeted inhibitors. Nat. Rev. Cancer. 5, 341–354.
Iqbal, N., Iqbal, N., 2014. Human epidermal growth factor receptor 2 (HER2) in cancers: overexpression and therapeutic implications. Mol. Biol. Int. 2014, 1–9.
John, S., Thangapandian, S., Sakkiah, S., Lee, K.W., 2010. Identification of potent virtual leads to design novel indoleamine 2,3-dioxygenase inhibitors: pharmacophore modeling and molecular docking studies. Eur. J. Med. Chem. 45, 4004–4012.
Johnston, S., Pippen, J., Pivot, X., Lichinitser, M., Sadeghi, S., Dieras, V., et al., 2009. Lapatinib combined with letrozole versus letrozole and placebo as first-line therapy for postmenopausal hormone receptor – positive metastatic breast cancer. J. Clin. Oncol. 27, 5538–5546.
Kallioniemi, O.P., Kallioniemi, A., Kurisu, W., Thor, A., Chen, L.C., Smith, H.S., et al., 1992. ERBB2 amplification in breast cancer analyzed by fluorescence in situ hybridization. Proc. Natl. Acad. Sci. 89, 5321–5325.
Kalous, O., Conklin, D., Desai, A.J., O'Brien, N.A., Ginther, C., Anderson, L., et al., 2012. Dacomitinib (PF-00299804), an irreversible pan-HER inhibitor, inhibits proliferation of HER2-amplified breast cancer cell lines resistant to trastuzumab and lapatinib. Mol. Cancer Ther. 11, 1978–1987.
Konecny, G.E., Pegram, M.D., Venkatesan, N., Finn, R., Yang, G., Rahmeh, M., et al., 2006. Activity of the dual kinase inhibitor lapatinib (GW572016) against HER-2-overexpressing and trastuzumab-treated breast cancer cells. Cancer Res. 66, 1630–1639.
Kute, T., Lack, C.M., Willingham, M., Bishwokama, B., Williams, H., Barrett, K., et al., 2004. Development of Herceptin resistance in breast cancer cells. Cytometry A 57, 86–93.
López-Tarruella, S., Jerez, Y., Márquez-Rodas, I., Neratinib, Martín M., 2012. (HKI-272) in the treatment of breast cancer. Future Oncol. 8, 671–681.
Lee-Hoeflich, S.T., Crocker, L., Yao, E., Pham, T., Munroe, X., Hoeflich, K.P., et al., 2008. A central role for HER3 in HER2-amplified breast cancer: implications for targeted therapy. Cancer Res. 68, 5878–5887.
Li, E., Hristova, K., 2006. Role of receptor tyrosine kinase transmembrane domains in cell signaling and human pathologies. Biochemistry 6241–6251.
Li, H., Sutter, J., Hoffman, R., 2000. HypoGen: an automated system for generating 3D predictive pharmacophore models. In: Guner, O. (Ed.), Pharmacophore Perception, Dev. Use Drug Des. SE – IUL Biotechnol. Ser.. International University Line, La Jolla, CA.
Li, J., Wang, H., Li, J., Bao, J., Wu, C., 2016. Discovery of a potential HER2 inhibitor from natural products for the treatment of HER2-positive breast cancer. Int. J. Mol. Sci. 2016.
Lipinski, C.A., 2004. Lead- and drug-like compounds: the rule-of-five revolution. Drug Discov. Today Technol. 337–341.
Liu, T., Lin, Y., Wen, X., Jorissen, R.N., Gilson Binding, M.K.D.B., 2007. A web-accessible database of experimentally determined protein-ligand binding affinities. Nucleic Acids Res. 35.
Lucas, F.A.M., Cristovam, S.N., 2016. HER2 testing in gastric cancer: an update. World J. Gastroenterol. 4619–4625.

Maximiano, S., Magalhães, P., Guerreiro, M.P., Morgado, M., 2016. Trastuzumab in the treatment of breast cancer. BioDrugs 30, 75–86.
Melvin, J.C., Wulaningsih, W., Hana, Z., Purushotham, A.D., Pinder, S.E., Fentiman, I., et al., 2016. Family history of breast cancer and its association with disease severity and mortality. Cancer Med. 5, 942–949.
Menderes, G., Bonazzoli, E., Bellone, S., Black, J.D., Lopez, S., Pettinella, F., et al., 2017. Efficacy of neratinib in the treatment of HER2/neu-amplified epithelial ovarian carcinoma in vitro and in vivo. Med. Oncol. 34, 91.
Miyamoto, S., Kollman, P.A., 1992. Settle: an analytical version of the SHAKE and RATTLE algorithm for rigid water models. J. Comput. Chem. 13, 952–962.
Olayioye, M a., 2001. Update on HER-2 as a target for cancer therapy: intracellular signaling pathways of ErbB2/HER-2 and family members. Breast Cancer Res. 3, 385–389.
Pannala, M., Kher, S., Wilson, N., Gaudette, J., Sircar, I., Zhang, S.-H., et al., 2007. Synthesis and structure–activity relationship of 4-(2-aryl-cyclopropylamino)-quinoline-3-carbonitriles as {EGFR} tyrosine kinase inhibitors. Bioorg. Med. Chem. Lett. 17, 5978–5982.
Parrinello, M., 1981. Polymorphic transitions in single crystals: a new molecular dynamics method. J. Appl. Phys. 52, 7182.
Rüschoff, J., Hanna, W., Bilous, M., Hofmann, M., Osamura, R.Y., Penault-Llorca, F., et al., 2012. HER2 testing in gastric cancer: a practical approach. Mod. Pathol. 25, 637–650.
Rampogu, S., Son, M., Park, C., Kim, H.-H., Suh, J.-K., Lee, K., 2017a. Sulfonanilide derivatives in identifying novel aromatase inhibitors by applying docking, virtual screening, and MD simulations studies. Biomed. Res. Int. 2017, 1–17.
Rampogu, S., Baek, A., Son, M., Zeb, A., Park, C., Kumar, R., et al., 2017b. Computational exploration for lead compounds that can reverse the nuclear morphology in progeria. Biomed. Res. Int. 2017, 1–15.
Rampogu, S., Baek, A., Zeb, A., Lee, K.W., 2018. Exploration for novel inhibitors showing back-to-front approach against VEGFR-2 kinase domain (4AG8) employing molecular docking mechanism and molecular dynamics simulationsBMC Cancer [Internet] 18, 264. . Available from: https://doi.org/10.1186/s12885-018-4050-1.
Rampogu, S., Rampogu Lemuel, M., 2016. Network based approach in the establishment of the relationship between type 2 diabetes mellitus and its complications at the molecular level coupled with molecular docking mechanism. Biomed Res. Int. 2016, 6068437 Hindawi Publishing Corporation.
Ronckers, C.M., Erdmann, C.A., Land, C.E., 2005. Radiation and breast cancer: a review of current evidence. Breast Cancer Res. 7, 21–32.
Ross, J.S., Slodkowska, E.A., Symmans, W.F., Pusztai, L., Ravdin, P.M., Hortobagyi, G. N., 2009. The HER-2 receptor and breast cancer: ten years of targeted anti-HER-2 therapy and personalized medicine. Oncologist 14, 320–368.
Sakkiah, S., Thangapandian, S., John, S., Kwon, Y.J., Lee, K.W., 2010. 3D QSAR pharmacophore based virtual screening and molecular docking for identification of potential HSP90 inhibitors. Eur. J. Med. Chem. 45, 2132–2140.
Schroeder, R.L., Stevens, C.L., Sridhar, J., 2014. Small molecule tyrosine kinase inhibitors of ErbB2/HER2/Neu in the treatment of aggressive breast cancer. Molecules 15196–15212.
Schwartzberg, L.S., Franco, S.X., Florance, A., O'Rourke, L., Maltzman, J., Johnston, S., 2010. Lapatinib plus letrozole as first-Line therapy for HER-2+ hormone receptor-Positive metastatic breast cancer. Oncologist 15, 122–129.
Shah, R., Rosso, K., 2014. Nathanson SD Pathogenesis, prevention, diagnosis and treatment of breast cancer. World J. Clin. Oncol. 5, 283–298.
Sierke, S.L., Cheng, K., Kim, H.H., Koland, J.G., 1997. Biochemical characterization of the protein tyrosine kinase homology domain of the ErbB3 (HER3) receptor protein. Biochem. J. 322 (Pt 3), 757–763.
Swain, S.M., Baselga, J., Kim, S.-B., Ro, J., Semiglazov, V., Campone, M., et al., 2015. Pertuzumab, trastuzumab, and docetaxel in HER2-positive metastatic breast cancer. N. Engl. J. Med. 372, 724–734.
Tareq Hassan Khan, M., 2010. Predictions of the ADMET properties of candidate drug molecules utilizing different QSAR/QSPR modelling approaches. Curr. Drug Metab. 11, 285–295.
Tazzite, A., Jouhadi, H., Saiss, K., Benider, A., Nadifi, S., 2013. Relationship between family history of breast cancer and clinicopathological features in Moroccan patients. Ethiop. J. Health Sci. 23, 150–157.
Van Der Spoel, D., Lindahl, E., Hess, B., Groenhof, G., Mark, A.E., 2005. Berendsen HJC. GROMACS. fast, flexible, and free. J. Comput. Chem. 1701–1718.
von Minckwitz, G., Procter, M., de Azambuja, E., Zardavas, D., Benyunes, M., Viale, G., et al., 2017. Adjuvant pertuzumab and trastuzumab in early HER2-positive breast cancer. N. Engl. J. Med. 377, 122–131.
Wu, Y., Zhang, D., Kang, S., 2013. Physical activity and risk of breast cancer: a meta-analysis of prospective studies. Breast Cancer Res. Treat. 137, 869–882.
Zanini, E., Louis, L.S., Antony, J., Karali, E., Okon, I.S., McKie, A.B., et al., 2017. The tumor suppressor protein OPCML potentiates Anti–EGFR and Anti–HER2 targeted therapy in HER2 positive ovarian and breast cancer. Mol. Cancer Ther. 16 2246 LP-2256.
Zhao, D., Wang, H., Lian, Z., Han, D., Jin, X., 2011. Pharmacophore modeling and virtual screening for the discovery of new fatty acid amide hydrolase inhibitors. Acta Pharm. Sin. B 1, 27–35.
Zoete, V., Cuendet, M.A., Grosdidier, A., Michielin, O., 2011. SwissParam: a fast force field generation tool for small organic molecules. J. Comput. Chem. 32, 2359–2368.